

Chemotaxis Behavior Mediated by Single Larval Olfactory Neurons in *Drosophila*

Elane Fishilevich, Ana I. Domingos, Kenta Asahina,
Félix Naef, Leslie B. Vosshall, and Matthieu Louis

Supplemental Experimental Procedures

Multiple Testing Adjustment with a Resampling-Based FDR Approach

For a given odor, let d_i denote the mean of the distance separating the i^{th} larva from the odor during a 5 min interval. Denote as M_{Or1a} the median of all the mean distances d_i recorded for animals with a single functional neuron expressing *Or1a*. Similarly, M_{Or42a} and M_{Or49a} stand for the medians of the mean distances recorded for larvae with a single functional neuron expressing *Or42a* and *Or49a*. $M_{Or1a/Or42a}$ and $M_{Or1a/Or49a}$ represent the medians corresponding to animals with a pair of functional neurons (*Or1a* and *Or42a*) and (*Or1a* and *Or49a*), respectively. For each genotype, we wanted to find the subset of odors for which the median of the distance distribution is significantly different from that of the negative controls.

Given the relatively large number of odors tested for each genotype, conducting univariate analysis of the difference between group medians by using significance levels not corrected for the multiple comparisons will create the risk of “false discoveries” (type I errors). To address this issue of multiple testing, one can control the overall probability of making at least one type I error in the family of tests (Family-Wise type I Error Rate, FWER) [S1]. Many procedures have been proposed for controlling the FWER. The Bonferroni adjustment procedure, the simplest and most stringent one, guarantees that the probability of making any false discovery is less than the designated significance level. Although the high level of stringency of the Bonferroni adjustment drastically increases the likelihood of false negatives (type II error), and thereby reduces the test power [S2], making no adjustments for multiple comparison is not an acceptable alternative. A reasonable compromise consists in controlling the rate of false discoveries [S3]. The approach applied here relies on a permutation-based resampling technique developed by Korn and colleagues [S4]: Consider the genotype γ tested against its appropriate negative control(s) (denoted as η_γ) for N different odors ($N = 53$). Let $\{p_1, p_2, \dots, p_N\}$ be the p values obtained from the univariate Wilcoxon rank-sum tests, and let $\{H_1, H_2, \dots, H_N\}$ denote the null hypotheses of the corresponding tests (H_j : genotype γ and controls η_γ are indistinctly attracted by the j^{th} odor). Consider now the multivariate permutation distribution of p values $\{\tilde{p}_1, \tilde{p}_2, \dots, \tilde{p}_N\}$ generated by (i) randomly permuting the label on the specimens in the N odor groups containing the samples γ and η_γ and by (ii) calculating the Wilcoxon test on the permuted data. Let π^1 be the smallest p values in the distribution. Similarly, let π^u be the u^{th} but smallest p value in this distribution. For the N odor groups, we generate K such random permutations and perform a Wilcoxon test. Let us denote the u^{th} but smallest p value found in the k^{th} permuted data set as $\pi^{u,k}$. Suppose now we want to be $(1 - \alpha)$ confident that the number of false discoveries is smaller or equal to the integer u . Let \tilde{q}_α^u denote the α quantile of the distribution corresponding to the u^{th} but smallest p values $\{\pi^{u,1}, \pi^{u,2}, \dots, \pi^{u,K}\}$. For odors $j = \{1, \dots, N\}$, we reject the null hypothesis H_j if $p_j < \tilde{q}_\alpha^u$. For a given u , the rate of false discoveries is equal to the number of false discoveries u divided by the total number of null hypotheses rejected. In the present paper, we treated the case $u = 0, 1$, and 2. Because the number of specimens in each sample is typically larger than 30, all the possible permutations could not be tested, and we calculated the \tilde{q}_α^u on the basis of 10^5 permutations. For multiple independent tests, the stringency of the traditional Bonferroni adjustment and the FDR resampling approaches are similar when zero false positives are tolerated [S4]. In Figure 4 in the main text, the critical α value adjusted upon Bonferroni correction is $0.05/53 = 9.4 \times 10^{-4}$. By comparison, the effective α values \tilde{q}_α^0 we obtain at a false-discovery rate of zero are comprised between 1.1×10^{-3} and 1.2×10^{-3} .

Multiple-Regression Model to Analyze Cases of Enhanced Chemotaxis

We tested the existence of combinatorial interactions between individual neurons on the basis of a multiple regression model. To determine whether larvae with two functional neurons are significantly more (or significantly less) attracted to a given odor than larvae with a single functional neuron, we used a linear model:

$$d_i = \beta_0 + \beta_1 \cdot \Gamma_{\text{one OR}} + \beta_2 \cdot \Gamma_{\text{two ORs}} + \varepsilon_i \quad (1)$$

where d_i denotes the distance of the i^{th} animal to the odor source; ε_i represents the residual; $\Gamma_{\text{one OR}}$ and $\Gamma_{\text{two ORs}}$ are binary indicators equal to 1 when the genotype has at least one or two functional neuron(s), respectively. The matrix representation of (1) is

$$\begin{pmatrix} d_1^{nc} \\ \vdots \\ d_n^{nc} \\ d_{n+1}^{\text{one OR}} \\ \vdots \\ d_{n'}^{\text{one OR}} \\ d_{n'+1}^{\text{two ORs}} \\ \vdots \\ d_{n''}^{\text{two ORs}} \end{pmatrix} = \begin{pmatrix} 1 & 0 & 0 \\ \vdots & \vdots & \vdots \\ 1 & 0 & 0 \\ \vdots & \vdots & \vdots \\ 1 & 1 & 0 \\ \vdots & \vdots & \vdots \\ 1 & 1 & 0 \\ \vdots & \vdots & \vdots \\ 1 & 1 & 1 \\ \vdots & \vdots & \vdots \\ 1 & 1 & 1 \end{pmatrix} \cdot \begin{pmatrix} \beta_0 \\ \beta_1 \\ \beta_2 \end{pmatrix} + \begin{pmatrix} \varepsilon_1^{nc} \\ \vdots \\ \varepsilon_n^{nc} \\ \varepsilon_{n+1}^{\text{one OR}} \\ \vdots \\ \varepsilon_{n'}^{\text{one OR}} \\ \varepsilon_{n'+1}^{\text{two ORs}} \\ \vdots \\ \varepsilon_{n''}^{\text{two ORs}} \end{pmatrix} \quad (2)$$

where d_i^{nc} denotes the distance of the i^{th} specimen among the negative controls, $d_i^{\text{one OR}}$ the distance of the i^{th} specimen among the single best rescue, and $d_i^{\text{two ORs}}$ the distance of the i^{th} specimen among the double rescue. From equation (1), one sees that enhanced chemotaxis (increase in attraction), which represents a potential case of synergism, will be associated with values of β_2 significantly smaller than 0. Inhibition (diminution in attraction) will be associated with values of β_2 significantly larger than 0. For the neurons expressing *Or1a* and *Or42a*, we first compare the medians M_{Or1a} and M_{Or42a} and retain the genotype showing the strongest attraction, say *Or42a*. Next, we estimate the regression coefficients β_0 , β_1 , and β_2 by the least-squares method with the data samples shown in (2): *Or83b^{-/-}*, *Or42a-Gal4/Or42a-Gal4;Or83b^{-/-}*, *UAS-Or83b/UAS-Or83b;Or83b^{-/-}* (negative controls); *Or42a-Gal4/UAS-Or83b;Or83b^{-/-}* (single best rescue); and *Or42a-Gal4/Or1a-Gal4;UAS-Or83b;Or83b^{-/-}* (double rescue). Finally, we test the null hypothesis, $H_0: \beta_2 \neq 0$, by computing the two-tail Student's statistic $t = \beta_2 / s_{\beta_2}$ where s_{β_2} is the standard error of the estimate β_2 [S5]. With a confidence $(1 - \alpha)$, the true value of the regression coefficient β_2 is comprised in the interval $\beta_2 \pm (t_{\alpha/2, \nu} \cdot s_{\beta_2})$ where ν is the residual degree of freedom. When the confidence interval does not contain zero, we conclude that the estimate β_2 is significant. In Figure S7A, the model (1) was applied with significance level 0.05 to identify potential cases of behavioral enhancement/inhibition for the *Or1a* and *Or42a* OSNs (left panel) and the *Or1a* and *Or49a* OSNs (right panel).

Multiple-Regression Model to Analyze Cases of Synergism

Having established the existence of enhanced chemotaxis for the OSNs expressing *Or1a* and *Or42a* and the four odors of Figure 5 and Figure S8, we tested whether the increase in attraction is additive, subadditive or superadditive by modifying the linear model (1) as follows:

$$d_i = \beta_0 + \beta_{Or1a} \cdot \Gamma_{Or1a} + \beta_{Or42a} \cdot \Gamma_{Or42a} + \beta_{Or1a/Or42a} \cdot \Gamma_{Or1a} \cdot \Gamma_{Or42a} + \varepsilon_i \quad (3)$$

where the binary indicator Γ_{Or1a} is equal to 1 when the *Or1a* OSN is functional and 0 otherwise. Similarly, Γ_{Or42a} is equal to 1 when the *Or42a* OSN is functional and 0 otherwise. The regression coefficients β are estimated by the least-squares method with the following data samples: *Or83b^{-/-}*, *Or1a-Gal4/Or1a-Gal4;Or83b^{-/-}*, *Or42a-Gal4/Or42a-Gal4;Or83b^{-/-}*, *UAS-Or83b/UAS-Or83b;Or83b^{-/-}* (negative controls); *Or1a-Gal4/UAS-Or83b;Or83b^{-/-}* (single *Or1a*-rescue); *Or42a-Gal4/UAS-Or83b;Or83b^{-/-}* (single *Or42a*-rescue), and

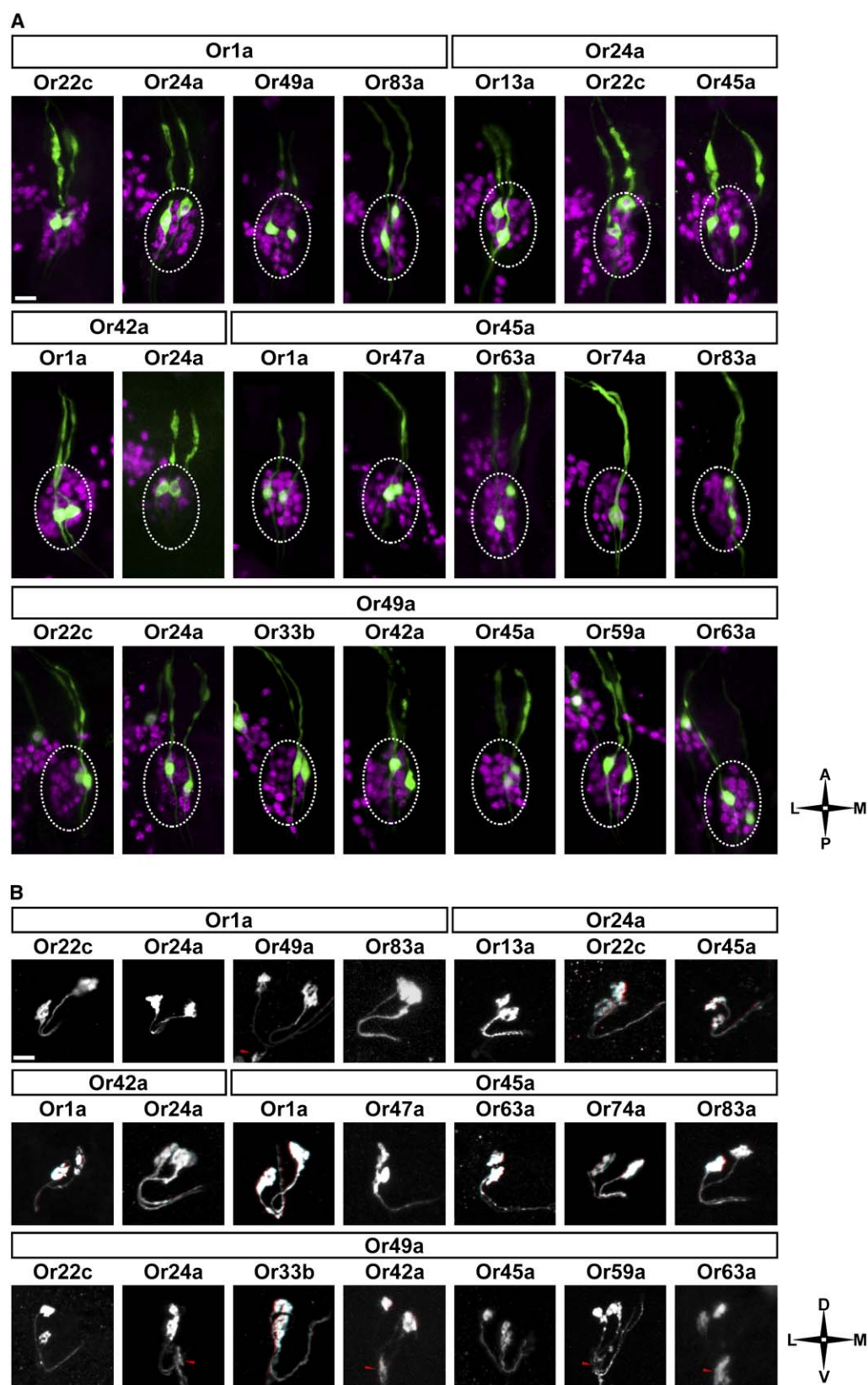


Figure S1. Organizational Logic of the Larval Dorsal Organ and Antennal Lobe

(A) Organizational logic of the larval dorsal organ. Whole-mount immunofluorescence preparations of *OrX-Gal4:OrY-Gal4:UAS-GFP* or *UAS-CD8-GFP* (green) are shown. Neuronal cell bodies in the dorsal-organ ganglion (white dashed circle) and the terminal organ are counterstained with *Elav* (9F8A9) antibody (magenta). Images are collapsed confocal Z stacks. The scale bar = 10 μ m. Orientation is as specified at lower right.

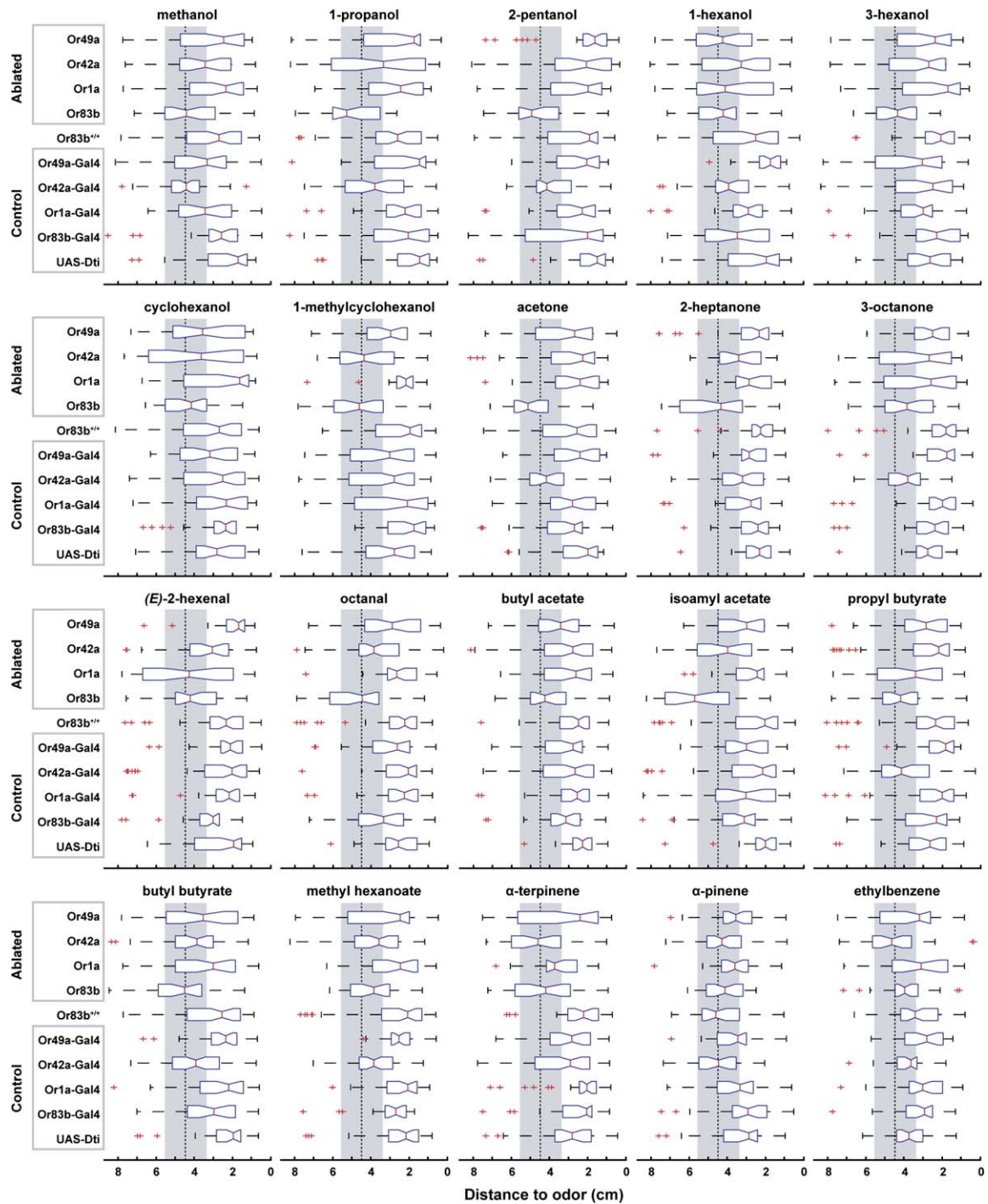


Figure S2. Box-Plot Representation of all Behavioral Data Obtained upon Genetic Ablation of Single Larval Sensory Neurons

Box plots of all behavioral data from Figure 3, including four ablated and five control genotypes tested with 2 μ l of 20 odor stimuli. Each plot consists of mean distances from the odor for animals measured over a 5 min trial. The median of the mean distance distribution corresponding to each genotype is indicated by the colored vertical line inside the box plot. Box boundaries represent the first and third quartiles, whiskers are 1.5 interquartile range, and outliers are indicated by red hatch marks. As a reference point, the median distance measured for 110 wild-type (yw) animals on a plate containing no odor stimulus is indicated by the dashed vertical line. The value of the first and third quartiles of this distribution forms the interval spanned by the gray shaded field. The ablations are of the *OrX/+;UAS-DTI/+* genotype. See Experimental Procedures for detailed genotypes.

(B) Organizational logic of the larval antennal lobe. Whole-mount immunofluorescence preparations of *OrX-Gal4::OrY-Gal4::UAS-GFP* or *UAS-CD8-GFP* animals. Images are collapsed confocal Z stacks. Terminal-organ projections of *Or49a-Gal4*-positive gustatory neurons are marked with a red arrowhead. The scale bar = 10 μ m. Orientation is as specified at lower right.

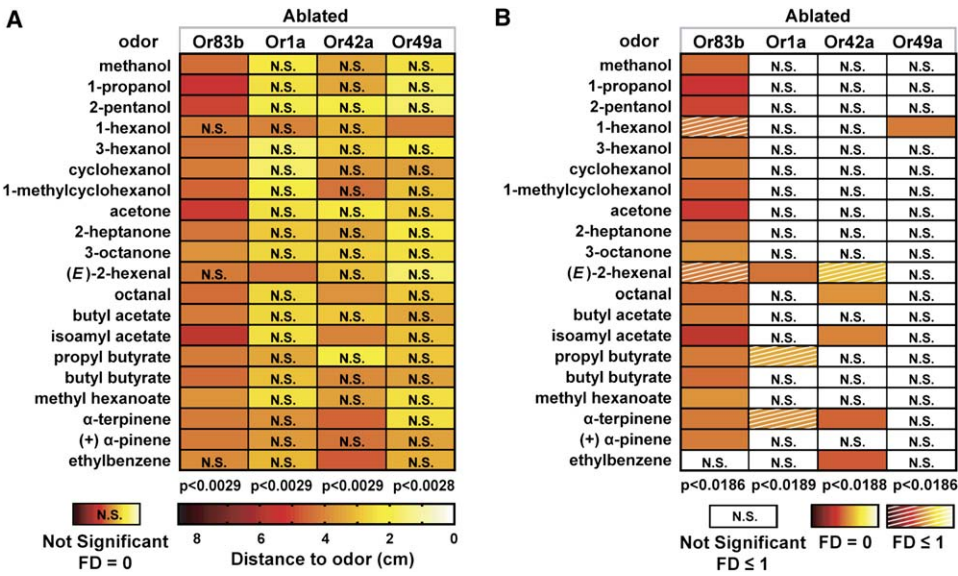


Figure S3. Summary of all Behavioral Data Obtained upon Genetic Ablation of Single Larval Sensory Neurons

(A) Unmasked summary of behavioral data for single neurons ablations from Figure 3 (in the main text) tested for 20 odor stimuli, at 2 μ l dose. For each odor and genotype, the median of the mean distance distribution is color-coded according to the scale shown at the bottom of the table. All cases with significantly impaired chemotaxis relative to controls (level 0.05; allowing zero False Discoveries [FD]) are masked with a white box labeled N.S. Corrected nominal significance levels for each genotype are listed at the bottom of each column.

(B) Summary of behavioral data to 20 odor stimuli presented at a dose of 2 μ l. For cases with significantly impaired chemotaxis relative to controls (level 0.05; allowing zero or one false discovery), distance-to-odor values are shown in plain (FD = 0) or with superimposed white hatch marks (FD \leq 1). All cases that do not meet these stringent statistical thresholds are masked with a white box labeled N.S. (not significant; level 0.05 and FD \leq 1). Corrected nominal significance levels for each genotype are listed at the bottom of each column.

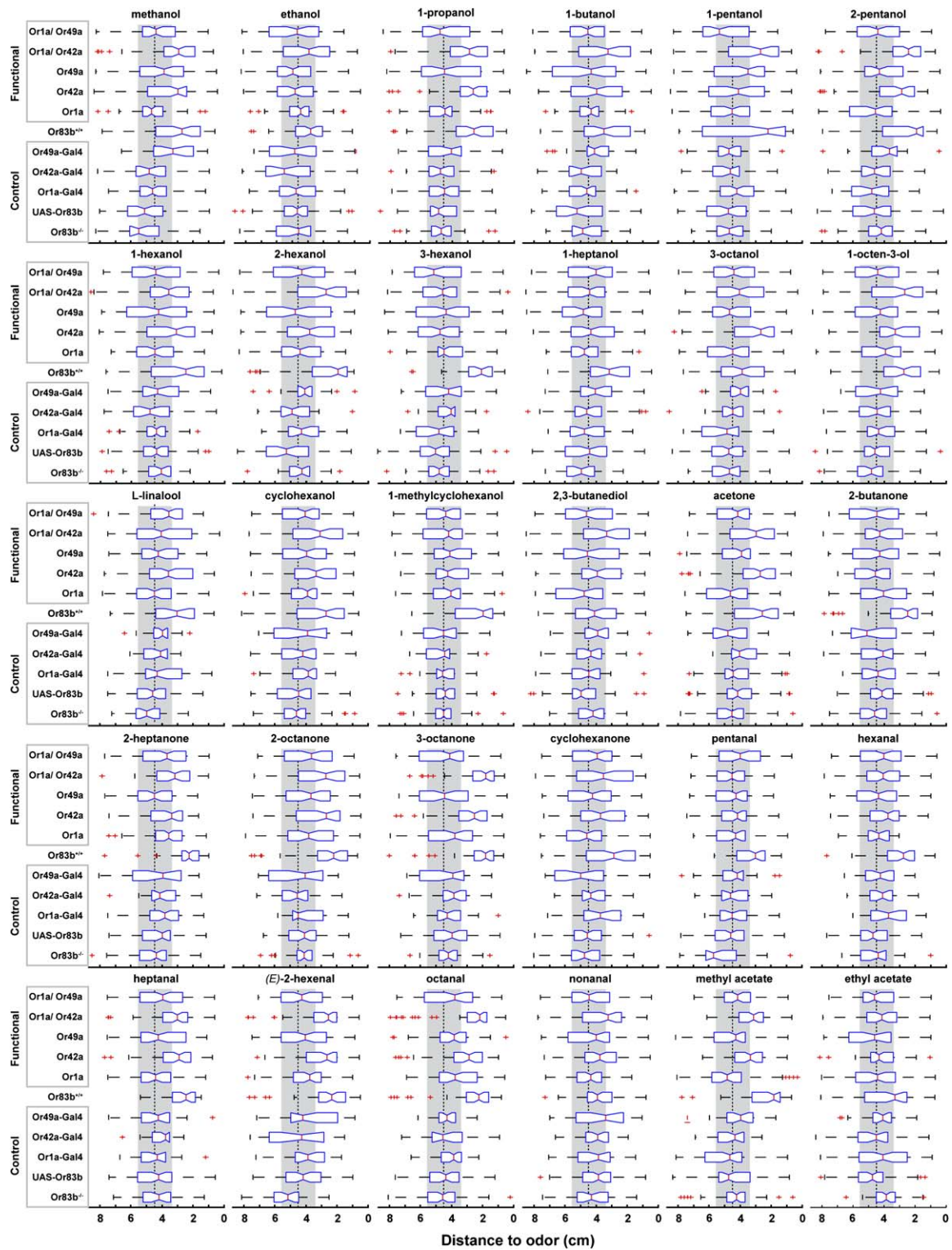


Figure S4. Box-Plot Representation of all Behavioral Data Obtained for Larvae with a Single Functional Olfactory Neuron: Part 1

Box plots of one and two functional OSN behavioral data from Figure 4, measured from six experimental and five control genotypes tested for 30 of the 53 odor stimuli, at a 2 μ l dose. Data are represented as discussed in Figure S2.

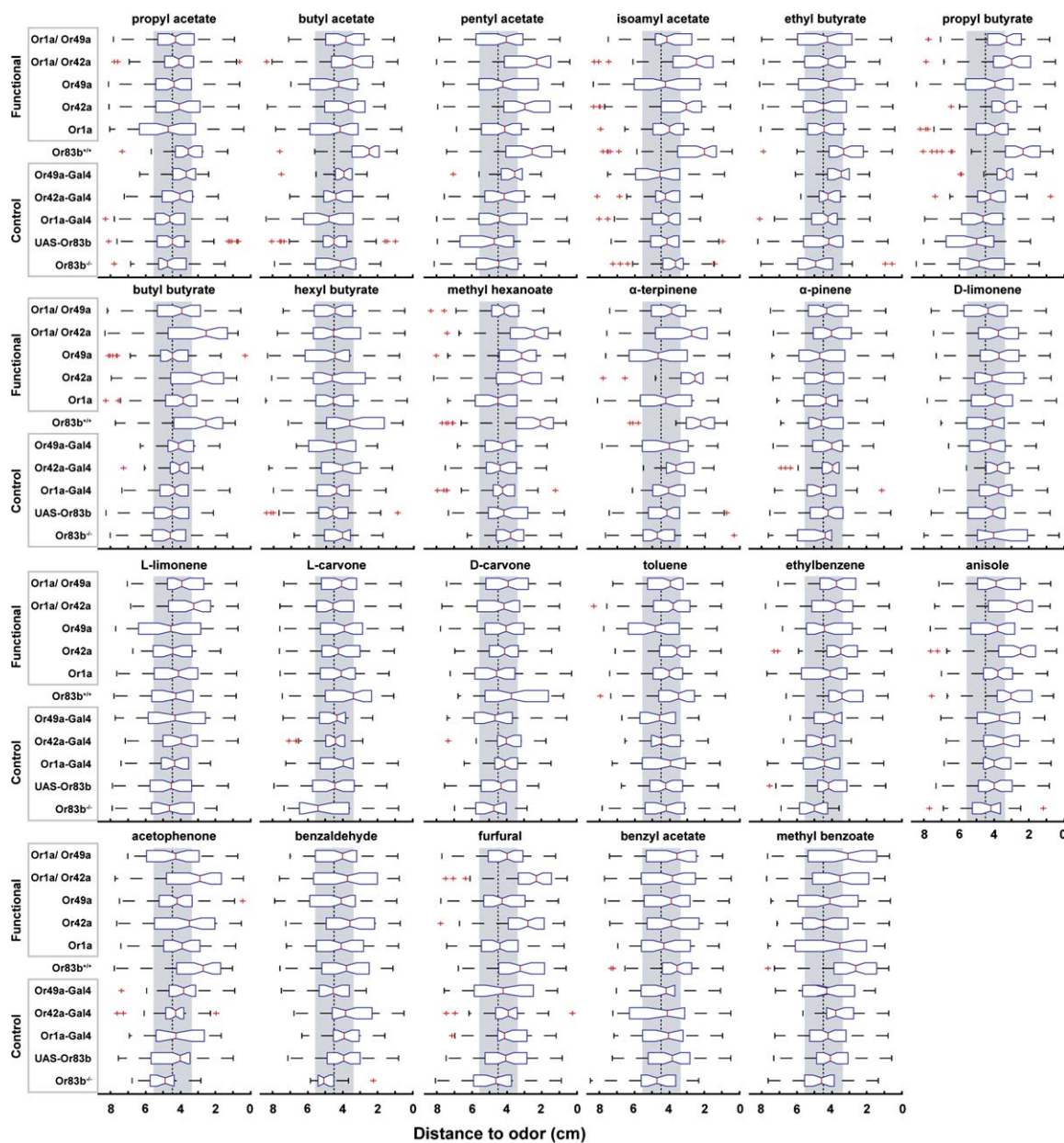


Figure S5. Box-Plot Representation of all Behavioral Data Obtained for Larvae with a Single Functional Olfactory Neuron: Part 2

Box plots of one and two functional OSN behavioral data from Figure 4 (in the main text) measured from six experimental and five control genotypes tested for the remaining 23 of 53 odor stimuli, at a 2 μ l dose. Data are represented as discussed in Figure S2.

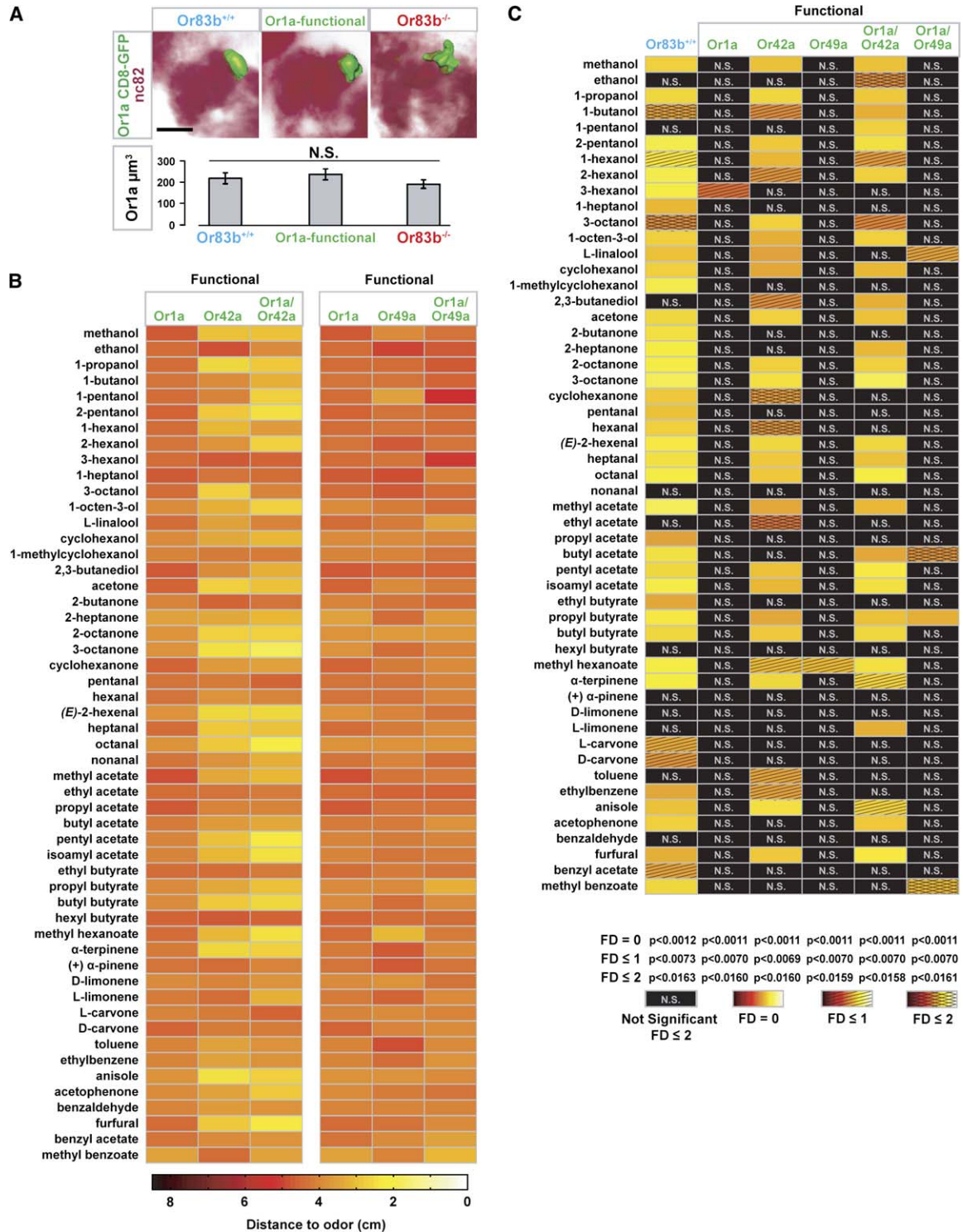


Figure S6. Or1a Glomeruli Volume and Summary of Behavioral Data Obtained for Larvae with a Single Functional Olfactory Neuron

(A) Surface view of the Or1a glomerulus in wild-type, Or1a-functional, and Or83b mutant backgrounds (green), along with a direct volume rendering of the larval antennal lobe stained with nc82 (dark red). Glomerular volume differences are not significant among these genotypes ($p > 0.2$; two-tailed t test). Mean volume \pm standard error of the mean (SEM), $n = 9$ animals, $n = 18$ glomeruli. The scale bar = 10 μm . In anosmic Or83b mutants, the Or1a glomerulus appears normal in approximately two-thirds of animals (data not shown) but shows stray fibers leaving the glomerulus in about one-third of animals (right panel). Three-dimensional Z-series of the GFP-labeled Or1a glomerulus in wild-type (Or1a-Gal4/UAS-CD8-GFP; TM2/+), Or1a-functional (Or1a-Gal4, UAS-Or83b/UAS-CD8-GFP; Or83b¹/Or83b²), and Or83b mutant animals (Or1a-Gal4/UAS-CD8-GFP; Or83b¹/Or83b²) were obtained by confocal microscopy. Images for all three genotypes were acquired under identical confocal settings. The volume of the Or1a glomerulus was measured with the segmentation software, Amira (TGS), with manual trimming of the afferent axon. Left and right glomeruli were averaged for each animal before the mean was calculated.

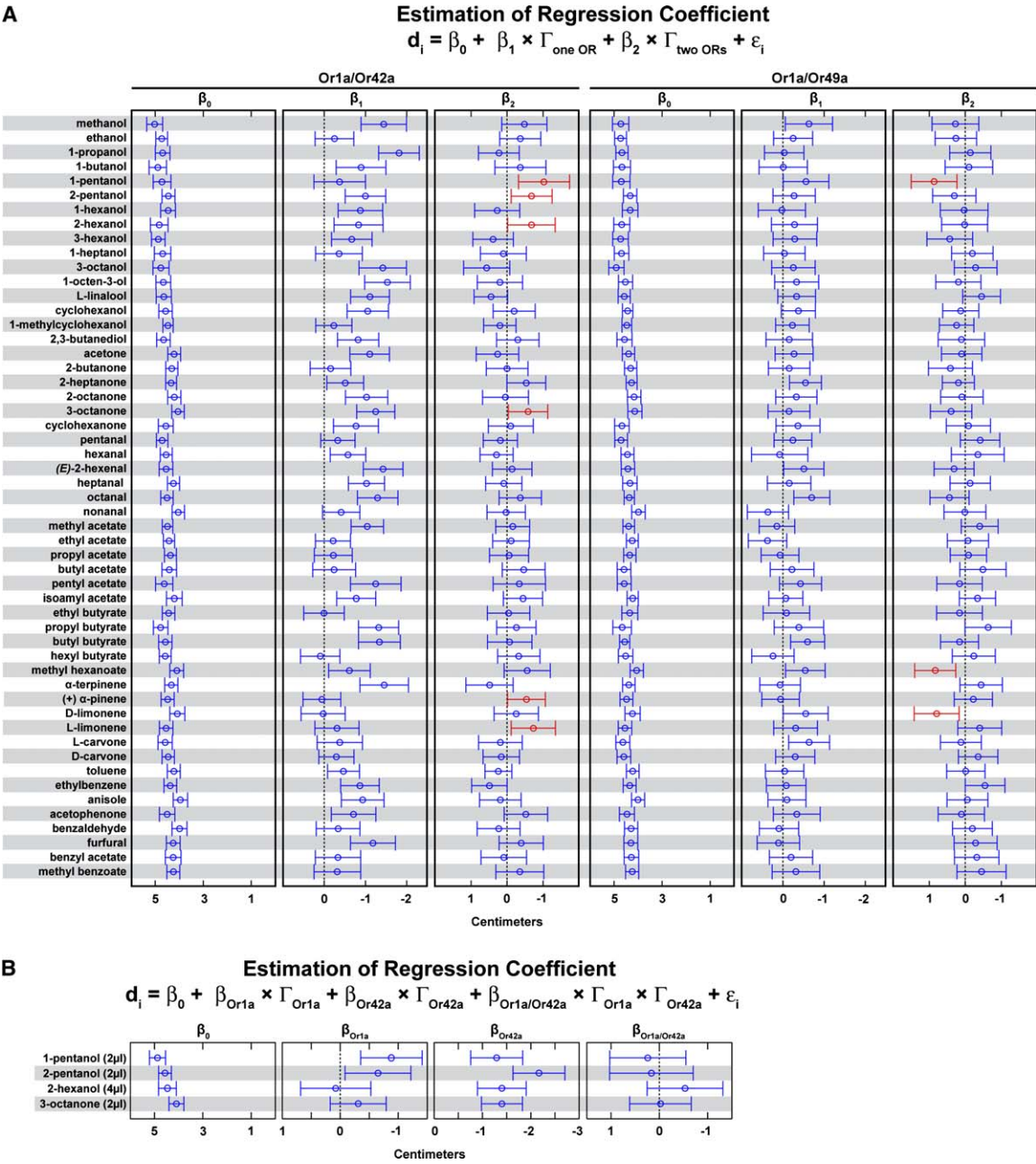


Figure S7. Application of the Regression Model Used to Detect Cases of Enhanced Chemotaxis

Estimation of the regression coefficients used in two linear models to compare the response profiles of larvae with one and two functional neurons (Figures 4, 5, S8).

(A) Exploratory model applied to 53 odors to identify cases of chemotaxis enhancement (or inhibition) between the double and the single functional genotypes. The model is based on a multiple-regression function for the distance to the odor shown at the top of the figure (for detailed explanations, see Supplemental Experimental Procedures). The graphics correspond to *Or1a/Or42a* (left) and *Or1a/Or49a* (right) functional

Figure S6 (continued) (B) Unmasked behavioral data from Figure 4 (in the main text) of larvae with one and two functional neurons tested with 2 µl for 53 different odor stimuli. For each odor, the median distance to odor corresponding to each genotype is indicated using the pseudo-color scale shown at the bottom of the table. Genotypes are grouped according to the pairs of functional neurons used in the experiments, *Or1a/Or42a* and *Or1a/Or49a*.

(C) Summary of all behavioral data from Figure 4 of larvae with one and two functional neurons to 53 odor stimuli at three different False Discovery (FD) levels: FD = 0, 1, and 2. Medians of the distance to odor color-coded according to the scale are shown at the bottom of the table. Cases of chemotaxis recovery compared to the anosmic parental controls are reported for a family-wise error rate smaller than 0.05 at FD = 0, 1, and 2. Significant differences at FD = 0 are represented by unmasked boxes. Significance at FD = 1 and 2 are represented by a singly hatched and doubly hatched boxes showing the median distance in background. Median distance to odor is color-coded according to the scale in (B). Cases that are not significant for $FD \leq 2$ are masked and labeled as N.S. (not significant at $FD \leq 2$). Corrected nominal significance levels obtained at different FD levels are listed at the bottom of each column.

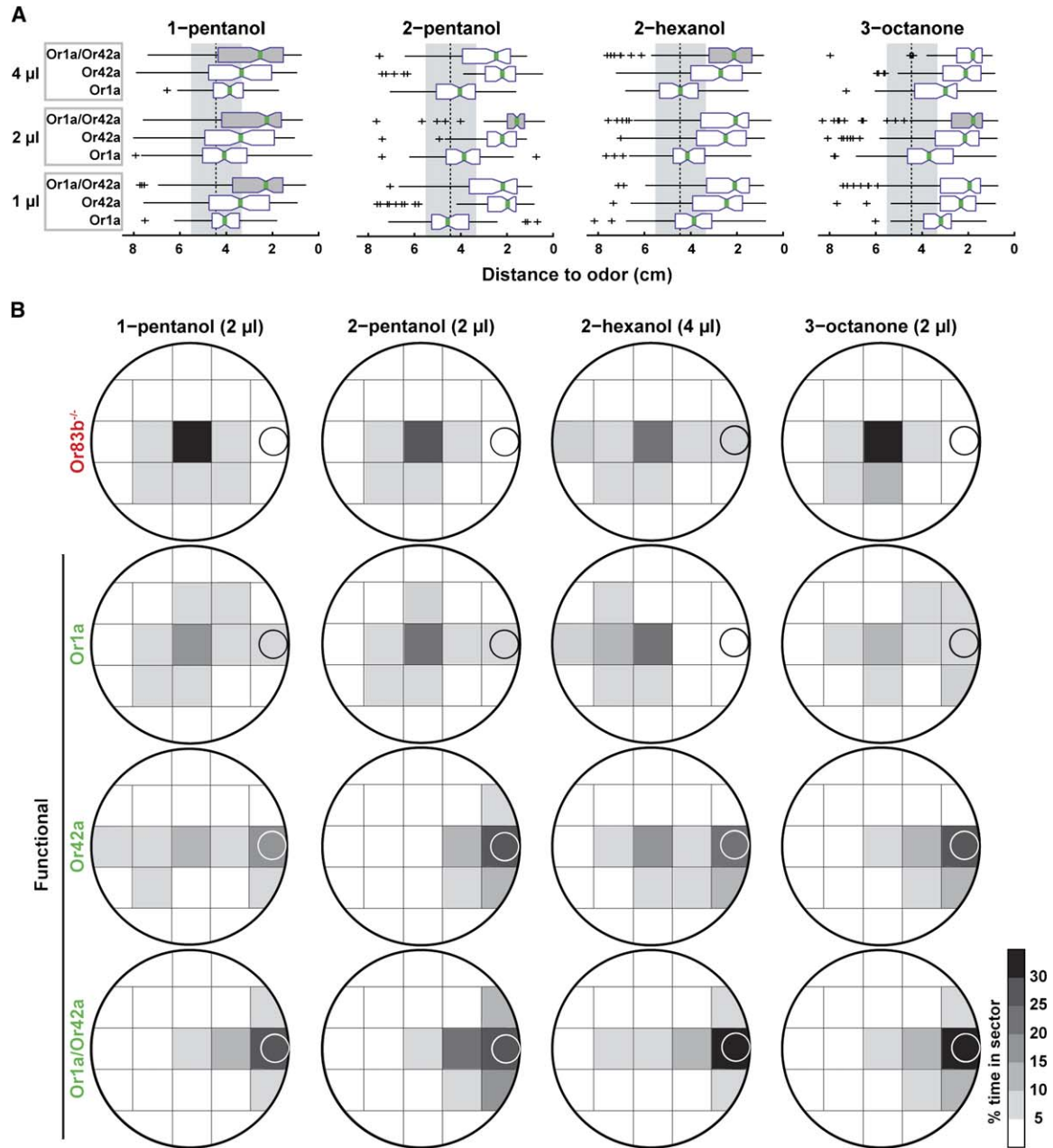


Figure S8. Chemotaxis Produced by Combinatorials of Functional Olfactory Neurons

Figure S7 (continued) OSNs. For each odor, the three regression coefficients β_0 , β_1 , and β_2 are estimated by the least-squares method (circles). The confidence interval on each estimate is represented by a horizontal bar calculated at a significance level 0.05. In six cases, *Or1a/Or42a*-functional is significantly different from single functional neurons (highlighted in red): 1-pentanol, 2-pentanol, 2-hexanol, 3-octanone, α -pinene, and L-limonene. For the above six odors except α -pinene, the p value of the overall regression is smaller than 0.0005. In each case, the value of β_2 is smaller than 0, reflecting an enhancement in chemotaxis. For the *Or1a/Or49a* OSNs, three cases of significant difference exist (right panel) and are highlighted in red: 1-pentanol, methyl hexanoate, and D-limonene. All three odors are associated with values of β_2 larger than 0, which reflect decreases in chemotaxis. However, none of these odors elicits a behavior that is significantly different between the one-/two-functional neurons and the parental controls (Figure 4). These three potential cases of inhibition were therefore not further investigated. In contrast, five out of the six odors eliciting chemotaxis enhancement are characterized by a behavior significantly different from the negative controls (Figure 4). In Figure 5 and Figure S8, we focused on four of these odors: 1-pentanol, 2-pentanol, 2-hexanol, and 3-octanone.

(B) Linear model applied to test whether the significant behavioral increases observed in Figure 5 and Figure S8 results from the synergistic interactions of the single OSNs. The regression equation used is shown on the top of the graphics and discussed in the Supplemental Experimental Procedures. Least-squares method was applied to estimate the regression coefficient at a significance level adjusted with the Bonferroni correction ($\alpha = 0.05/4$). As for panel A, the estimate of the regression coefficients and their confidence intervals are represented by a circle embedded in a horizontal bar. Because $\beta_{Or1a/Or42a}$ is not significantly different from 0 for any of 4 odors, we conclude that effects of the single neurons are not combined in a way that is more (or less) than additive.

Or42a-Gal4/Or1a-Gal4;UAS-Or83b;Or83b^{-/-} (double rescue). True cases of synergism where the enhancement in attraction characterizing the double rescue is greater than the sum of the attraction characterizing the single rescues will be associated to values of $\beta_{Or1a/Or42a}$ significantly smaller than 0. Conversely, cases where the relationship between the behavioral enhancement is less than additive will be reflected by values of $\beta_{Or1a/Or42a}$ significantly larger than 0. The result of the application of model (3) is shown in Figure S7B. Because no estimates of $\beta_{Or1a/Or42a}$ are significantly different from 0 ($p < 0.05/4$), we conclude that the combined effects of the *Or1a* and *Or42a* OSNs are not significantly greater than the sum of the individual contributions. This suggests that the behavioral enhancement observed for *Or1a/Or42a* does not meet the classical definition of synergy.

Supplemental References

- S1. Shaffer, J.P. (1995). Multiple hypothesis testing. *Annu. Rev. Psychol.* 46, 561–584.
- S2. Perneger, T.V. (1998). What's wrong with Bonferroni adjustments. *BMJ* 316, 1236–1238.
- S3. Dudoit, S., Yang, Y.H., Callow, M.J., and Speed, T.P. (2002). Statistical methods for identifying differentially expressed genes in replicated cDNA microarray experiments. *Statistica Sinica*. 12, 111–139.
- S4. Korn, E.L., Troendle, J.F., McShane, L.M., and Simon, R. (2004). Controlling the number of false discoveries: Application to high-dimensional genomic data. *J. Stat. Plan. Inference* 124, 379–398.
- S5. Zar, H.J. (1999). *Biostatistical Analysis*, Fourth Edition. (Upper Saddle River: Prentice Hall).

Figure S8 (continued) (A) Larvae exhibit enhanced chemotaxis to a concentration range of four odors when chemotaxis of animals with two neurons are compared with those having either single neuron alone. Box plots show chemotaxis data collected with 4 μ l, 2 μ l, or 1 μ l of stimulus. Significance was established by Wilcoxon rank-sum tests comparing data from the double functional neuron and the best single functional neuron larvae with Bonferroni correction for multiple comparisons ($p < 0.05/3$). In total, 3088 larvae were tested, mean $n = 87$ (range 47–165) per odor and genotype.

(B) Sector plots showing the averaged spatial distribution of animals from (A) for a single concentration of each odor.